Neuronal death induced by endogenous extracellular ATP in retinal cholinergic neuron density control

Valentina Resta[1], Elena Novelli[1], Francesco Di Virgilio[2] and Lucia Galli-Resta[1,*]

[1]Istituto di Neuroscienze CNR- 56100 Pisa, Italy
[2]Department of Experimental and Diagnostic Medicine, Section of General Pathology, and Interdisciplinary Center for the Study of Inflammation (ICSI), University of Ferrara, 44100 Ferrara, Italy
*Author for correspondence (e-mail: galli@in.cnr.it)

Accepted 6 April 2005

Development 132, 2873-2882
Published by The Company of Biologists 2005
doi:10.1242/dev.01855

Summary

The precise assembly of neuronal circuits requires that the correct number of pre- and postsynaptic neurons form synaptic connections. Neuronal cell number is thus tightly controlled by cell death during development. Investigating the regulation of cell number in the retina we found an ATP gated mechanism of neuronal death control. By degrading endogenous extracellular ATP or blocking the $P2X_7$ ATP receptors we found that endogenous extracellular ATP triggers the death of retinal cholinergic neurons during normal development. ATP-induced death eliminates cholinergic cells too close to one another, thereby controlling the total number, the local density and the regular spacing of these neurons.

Key words: Retina, Cell death, ATP, $P2X_7$, Amacrine cells, Mosaics, Rat

Introduction

In most brain regions, the number and relative density of neurons of each type vary remarkably little among individuals of the same animal strain (Williams and Herrup, 1988). This tight regulation controls the size of the different brain regions and allows the formation of proper neural connections.

Cell death plays a key role in regulating the number of neurons in the brain from its earliest stages of development. Death has been described among proliferating neuroblasts, early postmitotic cells and in many populations of neurons at the time they form synaptic connections (reviewed by Davies, 2003; de la Rosa and de Pablo, 2000; Lossi and Merighi, 2003; Oppenheim, 1991; Pettmann and Henderson, 1998). A long established idea is that the survival of developing neurons depends on trophic factors produced in limited amounts, but recent studies have shown that neuronal death may also partly be due to the activation of cytotoxic signaling mechanisms, through cell receptors such as FasL, TNF-R and P75 (reviewed in Davies, 2003; Dechant and Barde, 2002; Raoul et al., 2000).

A conserved mechanism of cell death activation has been described in non-neuronal cells (Falzoni et al., 1995; Girolomoni et al., 1993; Koshlukova et al., 1999), whereby extracellular ATP (e-ATP) triggers cell death by binding the $P2X_7$ receptors. Upon sustained or repeated activation, the $P2X_7$ receptors induce large non-selective membrane pores, which eventually lead to cell death (Di Virgilio et al., 1998; North, 2002).

$P2X_7$ receptors have been shown to be expressed in regions of the nervous system (North, 2002) and, therefore investigations were undertaken to determine whether endogenous e-ATP is involved in controlling the number and density of cells in specific neural populations. The retina is an ideal region to test this, since most of its neurons are arrayed with precisely controlled density, and there is a prominent expression of $P2X_7$. Among the developing retinal neurons, the cholinergic neurons seemed particularly relevant, because they are regularly spaced from early in development (Galli-Resta et al., 1997), and play a key role in normal development by triggering the waves of spontaneous neuronal impulse activity controlling the refinement of retinal projections to the brain (Wong, 1999).

We found that the retinal cholinergic cells express the $P2X_7$ receptors, and could be sources of endogenous e-ATP. Degrading e-ATP in vivo, or blocking the P2X receptors increases the density of the cholinergic neurons in the developing retina by preventing their naturally occurring death. This was also confirmed by directly monitoring e-ATP-induced death of individual cholinergic neurons in isolated retinas. Death induced by e-ATP in the retina is specific to the cholinergic neurons, normally removing cholinergic cells too close to one another, and thereby contributing to the regular density and spacing of these neurons.

Materials and methods

Animal and tissue treatment

Experiments were conducted on Long Evans hooded rats in accordance with national legislation and ARVO regulations. Animals were bred in the laboratory. Intraocular injections in newborns anaesthetized with ether were performed as described previously (Galli-Resta et al., 2002). Intraocular concentrations were determined assuming a 10 μl vitreal volume at P1, as previously estimated (Galli-Resta et al., 2002). Bromodeoxyuridine (BrdU), which is incorporated during DNA synthesis (Gratzner, 1982), was injected intraperitoneally (i.p.; 50 mg/kg body weight) every 6 hours starting immediately before the treatment in order to label all the cells entering S-phase after treatment. The S-phase in the retina is 12-18 hours at this

stage (Alexiades and Cepko, 1996). Animals were sacrificed by decapitation. Eye dissection, fixation, retinal flat-mounting or sectioning, and immunocytochemistry were performed as described previously (Galli-Resta and Ensini, 1996).

To control apyrase effectiveness in reducing e-ATP levels in vivo, we collected 5 μl fluid samples from the posterior eye chamber, reasoning that changes in ATP levels in this fluid would parallel those in the adjacent retina. P4 rats were anaesthetized with avertine (10 ml/kg body weight, i.p.; 3.3% tri-bromo-ethanol, 2% tertiary amyl-alcohol in saline) 3 hours after apyrase or vehicle intraocular injection. The tip (30-50 μm) of a glass micropipette connected to a 25 μl Hamilton syringe with a micro-driven piston was inserted into the posterior eye chamber. Samples were collected under a dissecting microscope to verify the lack of blood or opacity, and assayed in a luminometer (Perkin Elmer) to measure ATP levels by the luciferin-luciferase assay. Apyrase-treated animals showed a 50-fold reduction of e-ATP levels with respect to controls [2±1 μM vehicle injected (n=5 animals), 40±50 nM apyrase injected (n=5 animals), P<0.05, Student's t-test]. It is important to stress that these concentrations are lower than those found in the retina, where endogenous e-ATP reaches local concentrations around 0.1 mM (Newman, 2001). However, since it does not diffuse far (approx. 50 μm), and is rapidly degraded (Newman, 2001), its final concentration once diluted in the vitreus humor is much smaller.

Gene-gun labeling of explanted retinas

Imaging of living neurons was performed in retinas explanted from neonatal rats. Ages were uniformly distributed between P2 and P8. Retinas were quickly dissected in freshly made artificial cerebrospinal fluid (Stacy and Wong, 2003), flattened onto 13 mm Millipore nitrocellulose filters and placed in Petri dishes containing artificial cerebrospinal fluid (ACSF) within an oxygenated and humidified incubation chamber at room temperature (25-28°C). Individual cells were labeled with fluorescent-conjugated dextrans delivered by shooting dye-coated 1.3 μm tungsten particles into the retina using a Bio-Rad gene gun (Kettunen et al., 2002). Cholinergic cells were identified by their laminar positioning in the retina, their starburst morphology and their planar dendritic arrangement, which are already recognizable early in life (Stacy and Wong, 2003; Wong and Collin, 1989). In addition, we performed a morphological study combining YFP transfection to label individual cholinergic cells and immunohistochemistry for choline acetyltransferase (ChAT) to help identify the cholinergic cells in P2-P13 rat retinas (unpublished data). Gene-gun labeling with fluorescent dextrans produced an average of three to four labeled cholinergic neurons every 10 retinas, in accordance with the relatively low frequency of these neurons (Jeon et al., 1998).

Cell imaging in isolated retinas

Retinas were analyzed starting 1-2 hours after labeling. Cell images were obtained with a Zeiss Axioplan fluorescence microscope equipped with a black and white CCD camera (Chroma1600 DTA, Pisa, Italy). Retinas were placed on the microscope stage within a small observation chamber containing 4 ml of constantly oxygenated and frequently replaced ACFS maintained at room temperature.

Retinas were rapidly screened for labeled cholinergic cells using an Olympus 40× water immersion objective (NA 0.80), keeping excitation light at 10-20% of its maximum intensity. Two images were taken for each cell, focusing on the dendritic tree (3-second exposure), then on the soma (0.5-second exposure). After treatment, images were taken of the dendrites and the soma of previously recorded cells. Reference points within the observation chamber were recorded to identify specific cells in subsequent observations by means of their coordinates. To limit light exposure, treated and control cells were only imaged before and 30 minutes after treatment, unless otherwise specified. In some experiments, cells were transfected with YFP and similar results were obtained as with dextrans (not shown).

Membrane permeability was assessed by adding propidium iodide (PI; 1.5 μM, for 1 minute) to the ACSF. Exposure of phospatidylserine on the outer membrane leaflet was assessed with Cy3-annexin V (3 μg/ml, for 20 minutes). Images were acquired with the FITC (488 nm) filter setting for Oregon-Green-488-dextran, with the TRITC filter setting (568 nm) for PI, Cy-3-annexin V and Alexa-Fluo-568-dextran. Quinacrine (1 μM) was incubated for 10-20 minutes at room temperature and imaged using a Leica TCNS confocal microscope, keeping the laser at minimal power (5-10%). Since quinacrine easily bleaches, a maximum of two cells were scanned per retina, setting the scanning depth for each cell under the TRITC filter (displaying dextran labeling), then scanning with the FITC filter (quinacrine), and finally with the TRITC filter.

Data acquisition and analysis

The cholinergic cell arrays were sampled using a Leica TCNS confocal microscope. Four 400×400 μm^2 samples of either cholinergic cell arrays were taken in each whole-mount retina at mid-eccentricity along four perpendicular axes. The density of cholinergic cells does not vary with eccentricity at these ages (Galli-Resta et al., 2002). The same proved true in a dedicated analysis of the treated cases (eight samples per retina taken at two different eccentricities along four perpendicular axes, two retinas per treatment; not shown). Since in each case the objective was positioned midway between the papilla and the retinal margin without prior examination of the cell distribution, each sampling was unbiased. Sampled fields and retinal images were examined using an Image analyzer (Imaging Ontario, Canada) to determine cell density, cell positioning and retinal area. Cell counts and coordinates were obtained by feeding each sample field to the Imaging system and using an automatic cell counter based on intensity threshold and size exclusion criteria to eliminate noise. Total numbers of cells were estimated multiplying average cell density and retinal area. To investigate death among the cholinergic neurons, the sampled fields were screened for cellular debris retaining immunoreactivity for ChAT. ChAT-positive (ChAT+) debris within 15 μm of one another were counted as a single occurrence. Pycnotic cells in the GCL were counted in four samples (250×250 μm^2) per retina, after staining with propidium iodide. To sample non-cholinergic cells in the ganglion cell layer (GCL), whole-mount retinas were immunostained for ChAT (FITC: green), then labeled with PI (TRITC). The entire thickness of the GCL was scanned with a confocal microscope under the FITC+TRITC filter setting, taking eight samples (250×250 μm^2) per retina at two regularly spaced eccentricities along four perpendicular axes. All the PI cells that were not labeled for ChAT were then counted using Metamorph. Horizontal cells (tau-immunoreactive), dopaminergic amacrine [inner nuclear layer (INL) cells immunoreactive for tyrosine hydroxylase (TH)] and AII amacrine cells (Disabled 1 immunoreactive) were also counted: horizontal cells were sampled in four (400×400 μm^2) samples. TH cells were sampled in eight regularly spaced (400×400 μm^2) samples limited to the dorsotemporal retina where these cells are restricted early in life (Wu and Cepko, 1993); AII cells were sampled in four mid-eccentricity (250×250 μm^2) fields along four perpendicular axes.

Plots, frequency histograms and statistical analysis were made using Origin 7.0 (Microcal). Custom made programs were used to compute the autocorrelation, the density recovery profile (DRP), and the frequency of cells closer than 15 μm to one of their neighbors. The DRP and the exclusion radius (ER) are computed as follows. Concentric circles are traced at constant distances (here 2.5 μm) from one another in the autocorrelation, and a histogram (DPR) is obtained of the density of autocorrelation counts in the annuli delimited by two consecutive circles. The DRP values are very low close to the center of the autocorrelation (reflecting the central hole), and then rise to a final constant density in the bins far from the origin. The ER is obtained as the radius of the first circle (FC) where the histogram reaches or exceeds its average final density minus a correction weighing the autocorrelation counts found in the annuli contained

within FC. This correction is computed as the density of counts within the FC circle divided by the average DRP plateau value reached away from the origin, and multiplied for the histogram bin size (Rodieck, 1991). To evaluate the frequency of cell pairs with an intercellular distance below 15 µm, data from retinas treated with apyrase and oxidized ATP (oATP) were pooled together. The frequency of cell pairs was computed as the percentage of the total number of cell pairs in the field. In a field with n cells there are $n*(n–1)/2$ pairs of cells.

Reagents

Fluorescent conjugated dextrans (10 kDa, conjugated with Alexa Fluo 488 or 568 or Oregon Green 488), and fluorescent conjugated secondary antibodies were from Molecular Probes, Eugene, OR. Suramine was from Calbiochem. Antibodies to choline acethyltransferase (ChAT) and tyrosine hydroxylase (TH) were from Chemicon. The BrdU monoclonal antibody was from Roche. The $P2X_7$ polyclonal has been described previously (Ferrari et al., 1997); the A8 polyclonal to Islet 1/2 was a kind gift from T. Jessell; the antibody to Disabled 1 was a kind gift from B. Howell. All other chemicals were from Sigma.

Results

The rat retina has two arrays of cholinergic neurons, positioned in two separate layers (GCL and INL). To test whether e-ATP controls the death of these neurons during normal development, we injected postnatal day 1 (P1) rats intraocularly with blockers of the P2X purinergic receptors or with an ATP degrading enzyme, and analyzed the number of retinal cholinergic neurons in these animals 24 hours later (P2). Irreversible or slowly reversible agents were used because alterations in the rate of cell death must occur for some time to affect the total number of cells.

Extracellular ATP participates in the developmental control of the density and number of cholinergic amacrine cells

Neonatal rats subjected on P1 to intraocular injection of oxidized-ATP (oATP; 300 µM), an irreversible blocker of the P2X purinergic receptors (Murgia et al., 1993; North, 2002), displayed on P2 (i.e. 24 hours after the injection) a significant increase in the density of retinal cholinergic neurons (Fig. 1A,B). This was about 23% higher than normal for the cholinergic cells in the GCL, and 22% for the cholinergic cells in the INL (n=8 retinas; Fig. 1C,D). A similar density increase (+26% in the GCL, +28% in the INL; n=8 retinas) was observed 24 hours after intraocular injection of suramine (150 µM; Fig. 1C,D), a generic blocker of the purinergic P2 receptors (Ralevic and Burnstock, 1998), as well as after injections of apyrase (30 U/ml, +30% GCL, +21% INL; n=8 retinas; Fig. 1C,D), an enzyme that hydrolyses e-ATP (Komoszynski and Wojtczak, 1996). In all cases the increase in the density of cholinergic neurons was statistically significant (P<0.0001, t-test).

An increased cell density was not a generalized effect following e-ATP blockade, since we did not observe any change in retinal area (not shown), in the thickness of the retinal layers, or in the density of a number of cell populations that we analyzed as a control. These populations include the non-cholinergic cells in the GCL [mostly retinal ganglion cells at this age (Perry et al., 1983; Rabacchi et al., 1994)], the horizontal cells, the long-range dopaminergic amacrine cells and the short-range AII amacrine cells (Table 1; Fig. S1 in supplementary material).

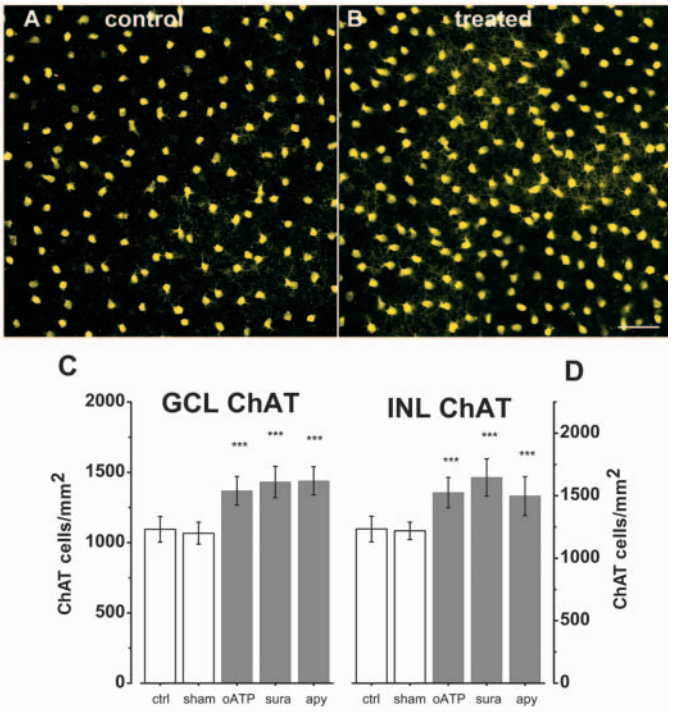

Fig. 1. Blocking e-ATP signaling in vivo increases the density of retinal cholinergic neurons in neonatal rats. (A) A sample of a control array of cholinergic (ChAT immunoreactive) neurons in the ganglion cell layer (GCL) of a P2 neonatal rat. (B) The density of cholinergic cells is increased 24 hours after in vivo treatment with oATP. Scale bar: 50 µm. (C,D) The density of cholinergic neurons in both the GCL (C) and the INL (D) is increased in vivo 24 hours after intraocular injection of oATP (an irreversible blocker of the P2X receptors), suramine (a blocker of the purinergic receptors), or apyrase (an eATP-degrading enzyme). Eight retinas were sampled per treatment. Data are displayed as means ± standard deviation. In all cases the increase in cholinergic cell density was statistically significant (P<0.0001, t-test). ctrl, normal control; sham, vehicle injected; oATP, oxidized-ATP injected; sura, suramine injected; apy, apyrase injected.

Since retinal areas were not affected by treatments blocking e-ATP signaling, the observed increase in the density of cholinergic neurons reflected true increments in the total number of these cells in both cholinergic arrays (Fig. 2A,B). An increase in the number of cholinergic cells was also observed 24 hours after treatments administered on P2 or P3 but not on P5 (Fig. 2A,B).

e-ATP causes death of the cholinergic neurons in normal retinal development

Since the cholinergic neurons found in treated retinas outnumbered the maximal number of these cells found in normal development (Fig. 2A,B), an accelerated migration of the cholinergic neurons to their layers could not account for the observed effects. New cell genesis was also excluded, since bromodeoxyuridine (BrdU), administered to label all the progenitor cells synthesizing DNA in the interval between treatment and analysis, was not detected in any of the 3000

Table 1. Blocking e-ATP signaling in vivo has no effects on a number of control retinal cell populations

Cell type (marker)	Vehicle injected (cells/mm^2)	e-ATP blockade (cells/mm^2)
RGCs (PI)	6120±360	6000±350 (oATP 300 μM) 6020±320 (apyrase 30 U/ml)
Horizontal cells (tau+)	960±60	1000±90 (oATP 300 μM)
Dopaminergic amacrine cells (TH+)*	136.9±4.5	135.2±4.5 (apyrase 30 U/ml)
AII amacrine cells (disabled+)	6426±300	6248±440 (apyrase 30 U/ml)

Intraocular injections were performed on P1 and the retinas analyzed on P2.

Cell counts were performed in whole-mount retinas, analyzing four retinas for each treatment and each cell type. In all cases, there is no significant difference between treated and control cases (*t*-test, $P<0.001$). See also Fig. S1 in the supplementary material.

*The TH cells were sampled in the dorso-temporal retina where these cells are restricted on P2 (Wu and Cepko, 1993).

cholinergic cells analyzed in sections from five treated retinas (Fig. 2C).

e-ATP can activate cell death in different non-neural cell populations (Di Virgilio et al., 1998). Investigations were therefore carried out to determine whether blocking e-ATP increased the number of cholinergic cells by preventing cell death among these neurons. In line with this hypothesis we found that cellular debris expressing cholinergic markers (ChAT+) had an average frequency of 3.7±1.4 every 1000 cholinergic cells in normal retinas (n=8 retinas), and decreased after e-ATP blockade, being 0.8±0.6 in oATP-treated retinas (n=8) and 0.7±0.6 in apyrase-treated retinas (n=8). This decrease was statistically significant ($P<0.001$, *t*-test) in both cases. Conversely, we observed up to a sixfold increase in the occurrence of ChAT+ debris (20±10 per 1000 cholinergic cells; n=3 retinas) 90 minutes after injection of 5 mM ATP into the eye. These changes in the frequency of ChAT+ cellular debris are consistent with the hypothesis that eATP regulates the basal level of cell death among the cholinergic neurons. e-ATP blockade did not affect the global occurrence of pycnotic cells in the GCL which was 6.5±2 every 1000 GCL cells in normal retinas (n=4) and 7.0±3 in oATP-treated retinas (n=4).

To test directly whether ATP kills the cholinergic neurons, we monitored the fate of individually labeled cholinergic cells after the application of ATP or other agents in isolated neonatal retinas aged between P2 and P8. Since experiments measuring endogenous e-ATP release in the rat retina have detected local eATP concentrations around 0.1 mM (Newman, 2001), we challenged cholinergic cells with this or higher concentrations of ATP. Developing cholinergic cells displayed dendritic and soma blebbing within minutes of ATP application (20/20 cells with 0.1 mM ATP; 5/5 cells with 0.5 mM ATP; 25/25 cells with 1 mM ATP; Fig. 3A-E). $P2X_7$ receptor activation induces membrane blebbing, membrane permeabilization to large cations such as propidium iodide (PI), and eventually leads to cell death (Di Virgilio et al., 1998; North, 2002). ATP-induced permeability to PI was observed in all individually identified cholinergic cells we tested (33/33 cells; Fig. 3F). Furthermore, Cy3-annexin V revealed phosphatidylserine exposure on the external leaflet of the cytoplasmic membrane (10/10 cells; right inset in Fig. 3C), a typical early indicator of the activation of a death process (Reutelingsperger et al., 2002).

Within 2-12 hours after ATP application the cell soma shrunk (8/8 cells; Fig. 3G). In most cases dendritic blebbing increased with time (e.g. Fig. 3A-C), then persisted for hours (3-12 hours) after ATP application. In a few cases, the cells shed their blebs and became very faint. 2′,3′-benzoyl-4-benzoyl-ATP (BzATP, 100 μM), a potent agonist at the $P2X_7$ receptors induced the same effects as did ATP, but with a faster dynamics, so that after extensive blebbing, all blebs were shed 30 minutes after application, leaving faintly labeled cells displaying intense PI nuclear staining (6/6 cells; not shown).

The effects of ATP application on the cholinergic cells were the same throughout the age range we tested (P2-P8; e.g. Fig.

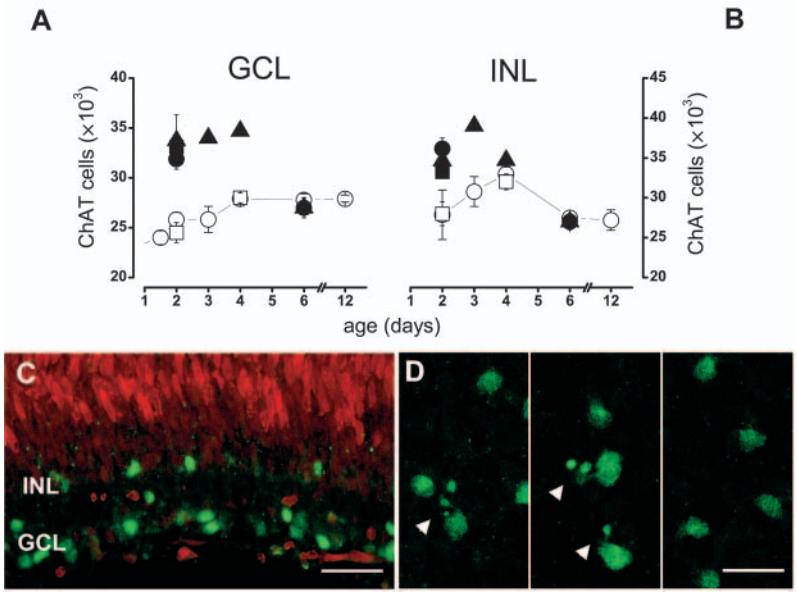

Fig. 2. e-ATP normally induces cell death in the developing population of cholinergic neurons. (A,B) Total number of cholinergic (ChAT) cells in the GCL (A) and the INL (B) 24 hours after in vivo treatment with apyrase (filled squares), suramine (filled triangles), or oATP (filled circles); control non-injected (open circles); vehicle-injected (open squares). The abscissa gives the age of analysis. The cholinergic cell number is increased if the treatment is administered between P1 and P3, but not on P5. Between 4 and 8 retinas were analyzed for each treatment and age point. (C) New cell genesis does not contribute to the increased number of cholinergic neurons, since BrdU (red) administered after the treatment does not label any cholinergic cells, identified here with an antibody to Islet-1/2 (green), which also labels retinal ganglion cells (Galli-Resta et al., 1997). Confocal image of a P2 retinal section. (D) Cellular debris immunoreactive for choline acetyltransferase can be observed in P2 whole-mount retinas 90 minutes after a shot of 5 mM ATP in the eye (left and central panel), while they are very rarely seen in normal P2 retinas (right panel). Scale bar: 50 μm in C; 20 μm in D.

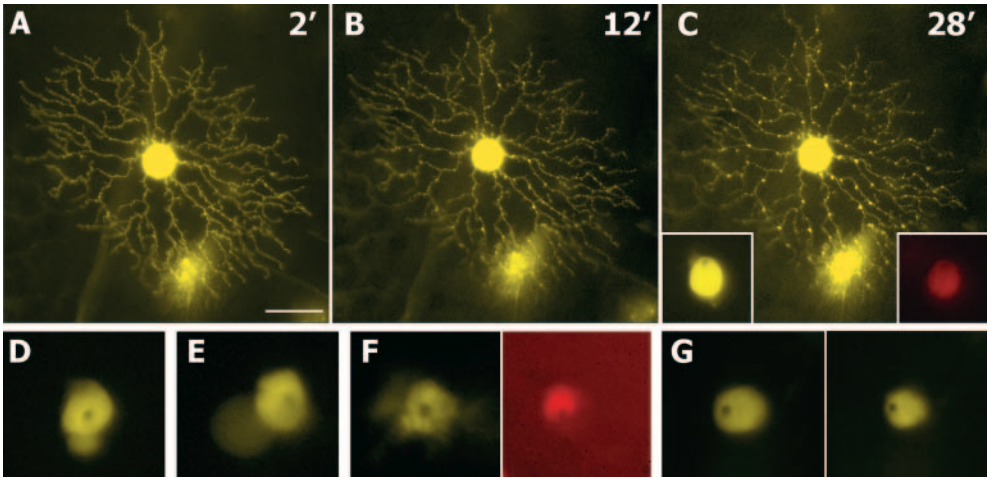

Fig. 3. Direct application of ATP to isolated neonatal retinas induces death of cholinergic neurons. (A-C) A P7 rat central retina cholinergic cell labeled with Alexa Fluor 488 dextran is illustrated at different times after application of 1 mM ATP. Small blebs in the dendritic tree are already apparent after a few minutes of ATP application (A), and become more conspicuous within 30 minutes. The cell soma (located in a different focal plane) displayed blebbing (left inset in C), and exposed phosphatidylserine on the outer membrane, as evidenced by Cy3-Annexin labeling (right inset in C). (D,E) Extensive soma blebbing was apparent in cholinergic neurons 30 minutes after application of 1 mM ATP (D) or 0.1 mM ATP (E). (F) In addition to blebbing (left) the cholinergic cells became permeable to propidium iodide (right), which displays a stronger fluorescence in the cell nucleus as a consequence of DNA binding (30 minutes after application of 1 mM ATP). (G) Between 2 hours and 12 hours after ATP application the soma of most cholinergic neurons lost their blebs and appeared shrunken (right panel) with respect to their original size (left panel). The small dark spot visible in D-G is the gene-gun bullet. Scale bar: 30 μm (A-C); 15 μm (insets in C); 10 μm (D-G). Images were acquired in black and white. By convention acquisition with the 488 nm emission filter (Alexa Fluo 488 dextran) are shown in yellow, acquisitions with the 568 nm emission filter (propidium iodide, Cy3-annexin) in red.

3A-F, Fig. 4A,B). Any detectable effect of ATP (1 mM) was prevented by the simultaneous incubation with apyrase (30 U/ml; 16/16 cells; Fig. 4C,D). Similarly, 2 hours of pre-incubation with the irreversible P2X antagonist oATP (300 μM) prevented blebbing and PI permeability (ATP 1 mM; 11/11 cells; Fig. 4E,F), even for ATP incubations as long as 2 hours. Finally, 30 minutes to 1 hour pre-incubation with Brilliant Blue G [BBG; a selective antagonist of rat $P2X_7$ when used below the micromolar range (North, 2002)], prevented blebbing and membrane permeability induced by ATP (1 mM

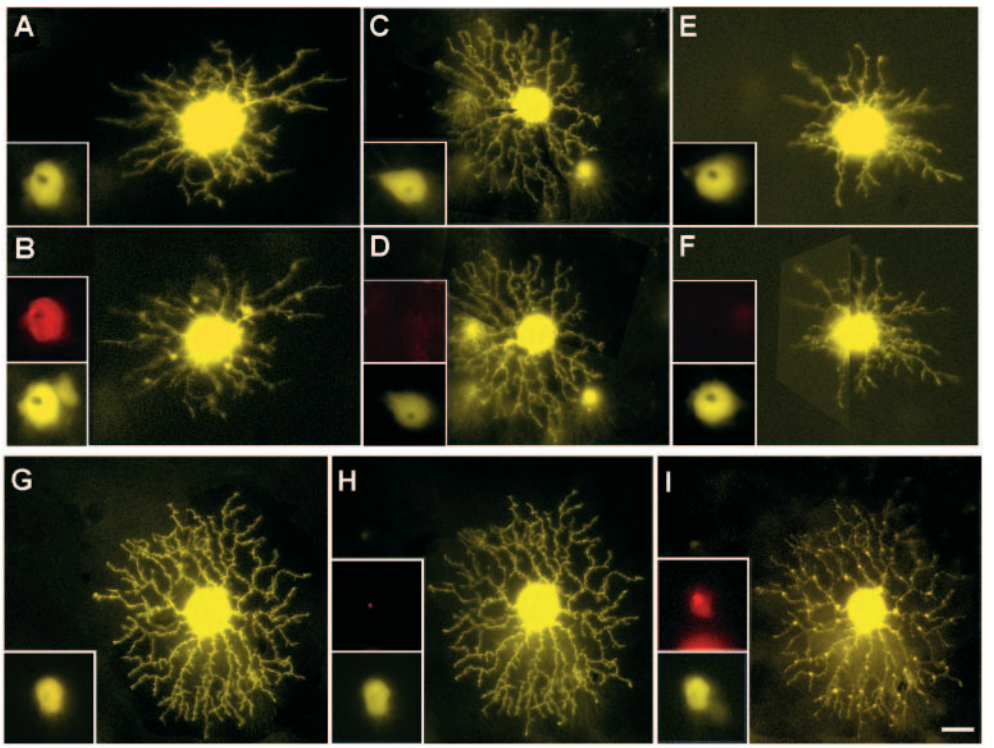

Fig. 4. Apyrase, oATP and BBG prevent ATP effects on individual cholinergic neurons in isolated retinas. (A,B) A P4 rat cholinergic cell before (A; cell soma in the inset) and 30 minutes after (B) application of 1 mM ATP. ATP induces extensive blebbing in the dendrites and soma (bottom inset in B), and permeability to PI (top inset in B). (C,D) A P5 rat cholinergic cell before (C, soma in inset), and 30 minutes after (D) application of 1 mM ATP in the presence of apyrase (30 U/ml). Apyrase totally prevented dendritic and somal blebbing (bottom inset in D), as well as PI permeability (top inset in D). (E,F) A P3 rat cholinergic cell preincubated with oATP (300 μM, 2 hours preincubation) is shown before (E) and 30 minutes after application of 1 mM ATP. Preincubation with oATP totally prevented dendritic and somal blebbing (bottom inset in F), as well as PI permeability (top inset in F). (G-I) A P5 rat cholinergic cell is shown just before (G, cell soma in the inset) and 30 minutes after (H) application of 1 mM ATP in the presence of 0.2 μM BBG. No blebbing is observed in the dendrites (H) or in the cell soma (bottom inset in H), nor was the cell permeable to PI (top inset in H; red dot is the gene gun bullet). The protective effect of BBG was reversible: after 10 minutes washing to remove BBG, application of 1 mM ATP induced blebbing of the cell dendrites (I) and soma (bottom inset in I), as well as cell permeability to PI (top inset in I) within 30 minutes. Scale bar: 15 μm (A-F); 8 μm (insets in A-F); 20 μm (G-I); 10 μm (insets in G-I).

for 30 minutes) in 95% of the tested cells (10/10 cells BBG 0.5 μM; 9/10 cells BBG 0.2 μM; Fig. 4G.H). The protective effects of BBG were reversible, since 1 mM ATP application after BBG washing induced membrane blebbing and permeabilization (5/5 cells BBG 0.5 μM; 5/5 cells BBG 0.2 μM; 10-minute washing followed by 1 mM ATP for 30 minutes; Fig. 4I). Membrane blebbing, loss of membrane integrity or annexin V labeling were never observed in 30 individually labeled cholinergic control cells, subjected to the same light exposure as the treated cells.

The cholinergic neurons express the $P2X_7$ receptor and are potential sources of e-ATP

The previous findings suggest that the $P2X_7$ receptors are a major pathway through which extracellular ATP triggers cholinergic cell death. Double immunostaining showed that the cholinergic cells express these receptors from P0 (Fig. 5A).

To search for e-ATP sources in the neonatal retina we used quinacrine, a vital green-fluorescent dye labeling high levels of ATP bound to peptides in large granular vesicles (Bodin and Burnstock, 2001). In P2-P8 rat retinas where individual cells had been labeled with Alexa-Fluo-564-dextran (red) to allow cell identification, we observed quinacrine labeling in the astrocytes of the central retina (not shown) and in all the cholinergic cells we had labeled (10/10 cells; Fig. 5B-D), while none of the individually labeled non-cholinergic amacrine cells or RGCs (0/25 cells) contained quinacrine (not shown). These data suggest (but do not prove) that the cholinergic cells could be endogenous sources of e-ATP in developing retinas, in accordance with previous observations (Santos et al., 1999).

Death induced by e-ATP eliminates cholinergic cells getting too close to one another

We reasoned that if the cholinergic cells were able to release e-ATP, e-ATP-induced death should mostly affect cholinergic cells close to one another, because e-ATP spreads only short distances (<50 μm) away from its source (Newman, 2001). In agreement with this prediction, we found a higher than normal frequency of cholinergic cells very close to one another after e-ATP blockade: while in vehicle injected control retinas the frequency of cholinergic cell pairs with an intercellular distance less than 15 μm is $2.7\times10^{-2}\pm0.8\times10^{-2}$, this frequency increased to $4.1\times10^{-2}\pm1\times10^{-2}$ in oATP- and apyrase-treated retinas ($P<10^{-5}$, *t*-test). To test this further we used the autocorrelation analysis, which plots the distances between all pairs of cells in an array. The autocorrelation of the cholinergic mosaics in normal or vehicle-injected retinas is a uniform distribution of points with a central empty region (e.g. Fig. 6A) (Galli-Resta, 2000). This means that each cholinergic cell normally tends to exclude other cholinergic neurons from a specific region surrounding its soma. Beyond this exclusion zone cholinergic cells can occupy any position in the field (Galli-Resta, 2000). The autocorrelations of the cholinergic mosaics treated with either oATP or apyrase differ from control simply because they have smaller empty regions (e.g. Fig. 6B), revealing a reduced efficacy of the exclusion mechanisms. This difference can be analyzed using the density recovery profiles (DRPs), histograms plotting the density of counts in the autocorrelation as a function of the distance from the center of the coordinates. In both control (example in Fig. 6C) and treated cases (Fig. 6D) the DRPs rise from zero to a constant density, but do so in much shorter distances in the treated than in the control cases. The size of the exclusion region is normally quantified using the exclusion radius (ER; arrows in Fig. 6C,D), which is calculated as the distance from the origin where the DRP reaches a constant density minus a correction factor considering the DRP counts at smaller distances [see Materials and methods and Rodieck (Rodieck, 1991)]. As shown in Fig. 6E, the average ER is reduced for the GCL cholinergic cell arrays treated with apyrase or oATP with respect to control. A similar ER reduction was observed for the INL cholinergic cell array after e-ATP blockade (not shown).

In summary, autocorrelation analysis shows that an increase in the frequency of cholinergic cells very close to one another is the major difference in the spacing of the cholinergic cells induced by e-ATP blockade. This means that e-ATP-induced death normally counteracts the occurrence of such close neighbors.

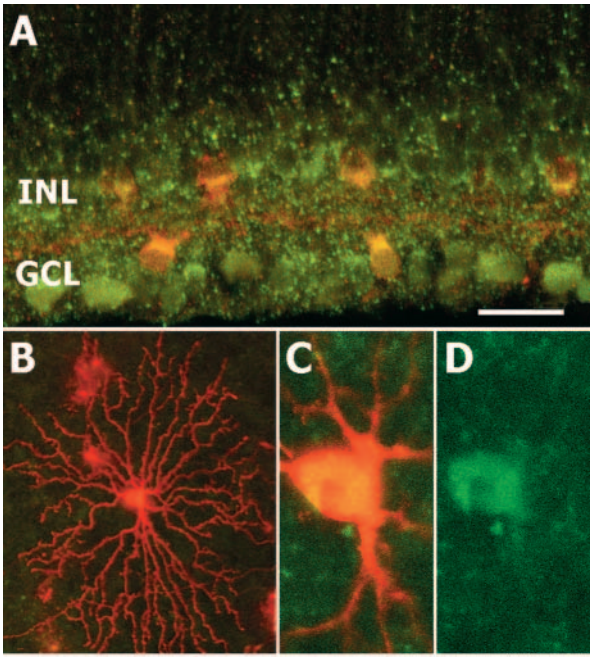

Fig. 5. The cholinergic neurons express the $P2X_7$ receptors and accumulate ATP in granules, which suggests that they could be sources of e-ATP. (A) In the neonatal rat retina the cholinergic cells (red) express the $P2X_7$ receptors (green), as do many retinal ganglion cells. Confocal image of a P4 retinal section. (B-D) Quinacrine, which labels high levels of ATP stored in granules, is found in the cholinergic cells. (B) Confocal image of a P8 rat cholinergic neuron labeled with Alexa Fluor 568 dextran. (C) A higher magnification of the same cell shows that its soma (red) contains quinacrine labeling (green), which is also shown in isolation in D. Scale bar: 20 μm (A); 40 μm (B); 10 μm (C,D).

Discussion

We have shown that degrading endogenous extracellular ATP (e-ATP) by intraocular injections of apyrase significantly increased the density and number of retinal cholinergic neurons in neonatal rats. The same effect was obtained with the purinergic antagonist suramine, or with oATP, a selective irreversible blocker of the P2X purinergic receptors (North,

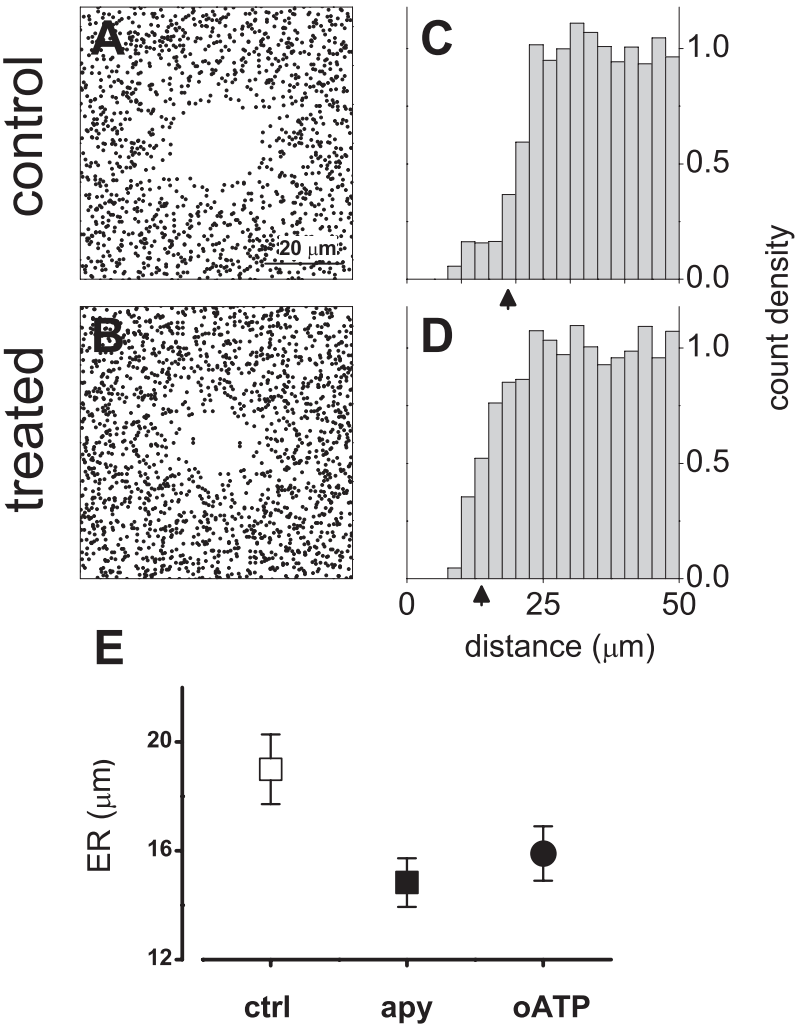

Fig. 6. Blocking e-ATP signaling increases the frequency of cholinergic cells not obeying the minimal spacing characteristic of these cells. (A) Autocorrelation plot of a normal cholinergic array at P2. The autocorrelation plots all the distances between the cells in the sample analyzed. In the normal cholinergic arrays the autocorrelation is a uniform distribution with a central hole. This means that the only spatial constraint these cells obey is to avoid getting closer to one another than a minimal distance, as already described (Galli-Resta et al., 1997). (B) Autocorrelation plot of an apyrase-treated cholinergic array at P2. The autocorrelation is still a uniform distribution with a central hole, but this is smaller than normal. This indicates the reduced efficacy of a mechanism normally ensuring the minimal spacing typical of the cholinergic arrays. (C,D) Examples of density recovery profiles (DRPs) histograms, plotting the density of counts in the autocorrelation as a function of the distance from the center of the coordinates, are shown for control (C) and treated (D) cells. In both cases the DRP rises from zero to a constant density, but does so in much shorter distances in the treated (D) than in the normal case (C). Count density is normalized to the average plateau density; an arrow indicates the exclusion radius (ER) value. (E) The size of the central exclusion region in the autocorrelation is quantified using the ER. The average ER is plotted with its standard deviation for the GCL cholinergic mosaics in control (vehicle injected) and apyrase- or oATP-injected retinas. e-ATP signaling blockade induces a significant ER reduction with respect to control (*t*-test, apyrase $P<10^{-7}$; oATP $P<10^{-6}$). Data were derived from the autocorrelation of all sampled fields (for each treatment $n=8$ retinas, 4 samples per retina).

2002). New cell genesis is excluded, since BrdU, which is incorporated into the DNA of proliferating cells, was not detected in any cholinergic neurons after e-ATP blockade. Accelerated cell migration is insufficient, as after e-ATP blockade we observed more cholinergic cells than are ever observed in the normal rat retina. Thus, e-ATP blockade must hamper a mechanism which normally reduces the number of cholinergic cells during development.

In principle the number of cholinergic cells can be reduced by inducing cell death among these neurons, or by promoting their trans-differentiation into a different type of cell, or by acting at both levels. Since e-ATP has been shown to trigger cell death in different non-neural cell populations (Di Virgilio et al., 1998) we first tested the effects of ATP on cholinergic cell death. In vivo we found that blocking e-ATP reduced the occurrence of cellular debris immunoreactive for cholinergic markers, while a pulse of exogenous ATP in the eye increased the cell debris. Furthermore, direct application of ATP in living isolated retinas rapidly induced clear signs of the activation of a death process in individually identified cholinergic neurons. These signs included membrane blebbing, loss of membrane integrity, exposure of phosphatidylserine on the external leaflet of the cytoplasmic membrane, and, finally, nuclear shrinkage. These effects were never reversible. Initially, we applied 1-0.5 mM ATP to isolated retinas, considering that the effective concentration at the tissue level was likely to be much lower, for the rapid degradation of ATP by endogenous ecto-nucleotidases (reviewed by Zimmermann, 1996). However, cholinergic cell death was also induced by 0.1 mM ATP, corresponding to typical concentrations observed close to the endogenous sources of ATP in the rat retina (Newman, 2001). The death-inducing effects of ATP were totally prevented by the simultaneous application of apyrase, which degrades e-ATP (Komoszynski and Wojtczak, 1996), or by preincubation with oATP, an irreversible P2X blocker (Murgia et al., 1993; North, 2002). Finally, Brilliant Blue G ensured total protection of 95% of the tested cells, at concentrations that selectively block the $P2X_7$ receptors (North, 2002). Taken together these data indicate that e-ATP can kill the cholinergic neurons, and does so during development.

The possibility that e-ATP could also control the cholinergic cell number by inducing a transdifferentiation of postmitotic cholinergic neurons into non-cholinergic cells was discounted. To our knowledge transdifferentiation of postmitotic neurons has never been observed in the retina, where cell fate appears to be determined around the time of the last cell division (Livesey and Cepko, 2001). Furthermore, we never observed any indication of mix-phenotypes (e.g. cells immunopositive

for ChAT but not displaying features typical of the cholinergic amacrine cells such as soma size, dendritic arrangement, planar organization, Islet immunoreactivity, or displaying features typical of non cholinergic cells) in vivo in normal retinas or after eATP blockade. Finally, direct application of ATP in concentrations normally observed in the rat retina (Newman, 2001) never induced anything but typical cell death indicators in individually labeled cholinergic cells in isolated retinas.

Future studies will be necessary to investigate the death process activated by e-ATP in the cholinergic neurons. Strong evidence points to $P2X_7$ as the most likely P2 receptor subtype responsible for the e-ATP cytotoxic effect, as suggested by the potent killing activity of BzATP, the protective effect of oATP and Brilliant Blue G, and the high level of expression of this receptor in the cholinergic neurons. This does not exclude the possibility that other P2X receptors for which a pore-forming ability has been demonstrated (e.g. P2X2 or P2X4) (Khakh et al., 1999; Virginio et al., 1999) might also be involved, although a death-inducing activity for P2X subtypes other than the $P2X_7$ has not been shown (North, 2002).

$P2X_7$ receptors have been shown to trigger both apoptosis and necrosis, depending on the cell type (Di Virgilio et al., 2001). In the retina we have been unable to label cholinergic cells using TUNEL or ISEL staining to detect fragmented DNA but these negative results may simply reflect the loss of cholinergic markers before these neurons reach advanced stages of death. More interestingly, we found that broad caspase inhibitors were unable to increase the number of cholinergic cells (not shown), suggesting that e-ATP induced a caspase-independent death.

Endogenous e-ATP as a local, possibly cell-type-specific cytotoxic agent for retinal cholinergic cells

Death induced by e-ATP in the developing retina appears specific to the cholinergic neurons. Blocking e-ATP signaling increased the number of cholinergic cells, but did not induce any generalized effect on retinal area, thickness or layering. Furthermore, treatments affecting e-ATP signaling did not alter cell density in a number of control cell populations. These include the horizontal cells, the short range amacrine cells AII, the long range dopaminergic amacrine cells, as well as all the non-cholinergic cells in the GCL (mostly retinal ganglion cells at these ages), notwithstanding most of these latter cells express the $P2X_7$ receptors (Fig. 5A) (Wheeler-Schilling et al., 2001). These results indicate that $P2X_7$ expression is not enough to make cells vulnerable to e-ATP-induced death, in line with previous results showing that susceptibility to ATP may depend on the level of expression of the $P2X_7$ receptors and the potential coupling of these receptors to cytoplasmic effectors (North, 2002). In addition, local e-ATP degradation by endogenous ecto-ATPases may selectively protect specific cells (Zimmermann, 1996), keeping endogenous e-ATP below the $P2X_7$ activation threshold around these cells. A similar reasoning may explain why we found that endogenous e-ATP controlled the death of cholinergic neurons only before P5, while direct ATP application could kill the cholinergic neurons also at later stages. Our preliminary data on the retinal distribution of the major ecto-ATPase (CD39) (Zimmermann, 1996) are consistent with this hypothesis, showing a concentration of CD39 around the ganglion cells between P0 and P5, and a much broader expression pattern afterwards (not shown).

Muller cells and astrocytes are sources of e-ATP in the adult retina (Newman, 2001; Newman, 2003), but in the first postnatal days Muller glia has not been generated yet (Wong and Godinho, 2003), and astrocytes are only found in the central retina (Ling et al., 1989). Therefore, we searched for e-ATP sources in the neonatal retina. Using quinacrine, a vital stain that binds ATP-containing vesicles, we found that the cholinergic cells store ATP in granules, which suggests that they are potential sources of e-ATP in the developing retina. Proving that the cholinergic cells do release ATP however, will require future studies.

Death induced by e-ATP controls the local density and regular spacing of the cholinergic neurons

We have found that the frequency of neighboring cholinergic cells spaced by less than 15 μm was higher than normal after e-ATP signaling blockade. In addition, autocorrelation analysis showed that the major effect of e-ATP blockade on the spacing of the cholinergic cells was a reduced efficacy of the mechanism by which each cholinergic cell normally excludes other cholinergic neurons from a limited region surrounding its soma. Thus, death induced by e-ATP not only controls the density of the cholinergic cells, but also contributes to the regular spacing that these neurons normally display in the retina. We do not know how this occurs, but we can propose a working explanation based on the assumption that the cholinergic cells release ATP: when two cell sources of e-ATP, which are both vulnerable to e-ATP-induced death, get too close to one another, if one or both release ATP, this can kill one, or even both of these cells, thereby reducing local overcrowding.

Most neurons in the retina form arrays, or mosaics, where cells of the same type are regularly spaced (Cook and Chalupa, 2000; Galli-Resta, 2002; Wässle and Riemann, 1978). This orderly arrangement of neurons of the same type is thought to ensure an even sampling of the visual field. Previous studies have shown that lateral cell displacement plays an important role in the formation of retinal mosaics (Galli-Resta et al., 1997; Reese and Galli-Resta, 2002; Reese et al., 1995), but simulation experiments (Jeyarasasingam et al., 1998) and studies of retinal mosaics in death-suppressing transgenic mice (Raven et al., 2003) strongly suggested that cell death also participates in this process. The present study provides direct evidence of a death control mechanism contributing to regular cell spacing and density in a neural population.

The selective elimination of cells too close to one another is a potent mechanism to prevent local overcrowding. However, cell death cannot by itself create a regular distribution of cells, unless a continuous provision of new cells is ensured until the final cell density and regular cell spacing are both achieved. This process would require an enormous amount of cell genesis, as simulation experiments easily show (e.g. simulating the formation of a normal cholinergic array by generating cells in random places and eliminating them whenever they do not obey the minimal spacing rule of 15±2 μm typical of the neonatal cholinergic arrays, shows that on average as many cells should be eliminated as finally remain in the array) (see also Eglen and Willshaw, 2002). This would not be the case, however, if cells too close to one another could also move apart: this process would reduce their risk of death, contribute to regular cell spacing, and reduce the number of new cells

necessary to achieve a final regular density. Tangential cell dispersion could in principle be enough to space cells appropriately, but we know little of the controlling mechanisms. Lateral cell migration has been shown to involve dendritic interactions (Galli-Resta et al., 2002), to be limited to a specific developmental time window, and to displace cells no more than 100-150 μm away from their clone of origin (reviewed by Reese and Galli-Resta, 2002). In several situations therefore, it might be more expedient for misplaced cells to die rather than move around till they are properly placed.

A dynamic regulation of cell number during cholinergic cell development

We have found that blocking for 24 hours the e-ATP-induced death of retinal cholinergic neurons in vivo significantly increases the total number of these cells (Fig. 2A,B). This means that many cholinergic neurons are normally dying at these ages. However, new cholinergic cells are also observed to migrate to the cholinergic arrays at these same times (Galli-Resta, 2000; Galli-Resta et al., 1997). The total number of cholinergic neurons reflects the balance between these two opposite contributions. This is not the first example of a cell population simultaneously undergoing cell death and cell replacement in the developing nervous system. This dynamic behavior has already been shown in the early development of retinal ganglion cells (Frade et al., 1997; Frade et al., 1996), in the avian ciliary ganglion (Lee et al., 2001) and in populations of retinal and cortical neuroblasts (reviewed by de la Rosa and de Pablo, 2000). The simultaneous presence of cell death and new cell addition makes it very difficult to estimate the real amount of cell death going on during development, or even to detect cell death as a decrease in the total number of cells.

Death induced by e-ATP has never been reported in the developing nervous system. However, a number of non neuronal cell populations, ranging from human macrophages (Falzoni et al., 1995) and keratynocytes (Girolomoni et al., 1993) to colonies of fungi (Koshlukova et al., 1999) undergo cell death induced by ATP through the $P2X_7$ receptors, suggesting that the cholinergic neurons are a new example of an ancient mechanism of cell death control.

We wish to thank G. C. Cappagli for invaluable technical support, R. O. L. Wong, M. Matteoli, C. Verderio, E. Strettoi, S. Eglen and A. Fiorentini for useful suggestions. A. Solini and E. Santini for help using the luminometer. This work was supported by the CNR, Murst FIRB and FISR.

Supplementary material

Supplementary material for this article is available at
http://dev.biologists.org/cgi/content/full/132/12/2873/DC1

References

Alexiades, M. R. and Cepko, C. (1996). Quantitative analysis of proliferation and cell cycle length during development of the rat retina. *Dev. Dyn.* **205**, 293-307.

Bodin, P. and Burnstock, G. (2001). Evidence that release of adenosine triphosphate from endothelial cells during increased shear stress is vesicular. *J. Cardiovasc. Pharmacol.* **38**, 900-908.

Cook, J. E. and Chalupa, L. M. (2000). Retinal mosaics: new insights into an old concept. *Trends Neurosci.* **23**, 26-34.

Davies, A. M. (2003). Regulation of neuronal survival and death by extracellular signals during development. *EMBO J.* **22**, 2537-2545.

de la Rosa, E. J. and de Pablo, F. (2000). Cell death in early neural development: beyond the neurotrophic theory. *Trends Neurosci.* **23**, 454-458.

Dechant, G. and Barde, Y. A. (2002). The neurotrophin receptor p75(NTR): novel functions and implications for diseases of the nervous system. *Nat. Neurosci.* **5**, 1131-1136.

Di Virgilio, F., Chiozzi, P., Falzoni, S., Ferrari, D., Sanz, J. M., Venketaraman, V. and Baricordi, O. R. (1998). Cytolytic P2X purinoceptors. *Cell Death Differ.* **5**, 191-199.

Di Virgilio, F., Chiozzi, P., Ferrari, D., Falzoni, S., Sanz, J. M., Morelli, A., Torboli, M., Bolognesi, G. and Baricordi, O. R. (2001). Nucleotide receptors: an emerging family of regulatory molecules in blood cells. *Blood* **97**, 587-600.

Eglen, S. J. and Willshaw, D. J. (2002). Influence of cell fate mechanisms upon retinal mosaic formation: a modelling study. *Development* **129**, 5399-5408.

Falzoni, S., Munerati, M., Ferrari, D., Spisani, S., Moretti, S. and Di Virgilio, F. (1995). The purinergic P2Z receptor of human macrophage cells. Characterization and possible physiological role. *J. Clin. Invest.* **95**, 1207-1216.

Ferrari, D., Chiozzi, P., Falzoni, S., Dal Susino, M., Collo, G., Buell, G. and Di Virgilio, F. (1997). ATP-mediated cytotoxicity in microglial cells. *Neuropharmacol.* **36**, 1295-1301.

Frade, J. M., Rodriguez-Tebar, A. and Barde, Y. A. (1996). Induction of cell death by endogenous nerve growth factor through its p75 receptor. *Nature* **383**, 166-168.

Frade, J. M., Bovolenta, P., Martinez-Morales, J. R., Arribas, A., Barbas, J. A. and Rodriguez-Tebar, A. (1997). Control of early cell death by BDNF in the chick retina. *Development* **124**, 3313-3320.

Galli-Resta, L. (2000). Local, possibly contact-mediated signalling restricted to homotypic neurons controls the regular spacing of cells within the cholinergic arrays in the developing rodent retina. *Development* **127**, 1499-1508.

Galli-Resta, L. (2002). Putting neurons in the right places: local interactions in the genesis of retinal architecture. *Trends Neurosci.* **25**, 638-643.

Galli-Resta, L. and Ensini, M. (1996). An intrinsic limit between genesis and death of individual neurons in the developing retinal ganglion cell layer. *J. Neurosci.* **16**, 2318-2324.

Galli-Resta, L., Resta, G., Tan, S.-S. and Reese, B. (1997). Mosaics of Islet-1 expressing amacrine cells assembled by short range cellular interactions. *J. Neurosci.* **17**, 7831-7838.

Galli-Resta, L., Novelli, E. and Viegi, A. (2002). Dynamic microtubule-dependent interactions position homotypic neurones in regular monolayered arrays during retinal development. *Development* **129**, 3803-3814.

Girolomoni, G., Santantonio, M. L., Pastore, S., Bergstresser, P. R., Giannetti, A. and Cruz, P. D., Jr (1993). Epidermal Langerhans cells are resistant to the permeabilizing effects of extracellular ATP: in vitro evidence supporting a protective role of membrane ATPase. *J. Invest. Dermatol.* **100**, 282-287.

Gratzner, H. G. (1982). Monoclonal antibody to 5-bromo and 5-iododeoxyuridine: a new reagent for detection of DNA replication. *Science* **381**, 474-475.

Jeon, C.-J., Strettoi, E. and Masland, R. (1998). The major cell populations of the mouse retina. *J. Neurosci.* **18**, 8936-8946.

Jeyarasasingam, G., Snider, C. J., Ratto, G.-M. and Chalupa, L. M. (1998). Activity regulated cell death contributes to the formation of ON and OFF α ganglion cell mosaics. *J. Comp. Neurol.* **394**, 335-343.

Kettunen, P., Demas, J., Lohmann, C., Kasthuri, N., Gong, Y., Wong, R. O. and Gan, W. B. (2002). Imaging calcium dynamics in the nervous system by means of ballistic delivery of indicators. *J. Neurosci. Methods* **119**, 37-43.

Khakh, B. S., Bao, X. R., Labarca, C. and Lester, H. A. (1999). Neuronal P2X transmitter-gated cation channels change their ion selectivity in seconds. *Nat. Neurosci.* **2**, 322-330.

Komoszynski, M. and Wojtczak, A. (1996). Apyrases (ATP diphosphohydrolases, EC 3.6.1.5): function and relationship to ATPases. *Biochim. Biophys. Acta* **1310**, 233-241.

Koshlukova, S. E., Lloyd, T. L., Araujo, M. W. and Edgerton, M. (1999). Salivary histatin 5 induces non-lytic release of ATP from Candida albicans leading to cell death. *J. Biol. Chem.* **274**, 18872-18879.

Lee, V. M., Smiley, G. G. and Nishi, R. (2001). Cell death and neuronal

replacement during formation of the avian ciliary ganglion. *Dev. Biol.* **233**, 437-448.
Ling, T. L., Mitrofanis, J. and Stone, J. (1989). Origin of retinal astrocytes in the rat: evidence of migration from the optic nerve. *J. Comp. Neurol.* **286**, 345-352.
Lossi, L. and Merighi, A. (2003). In vivo cellular and molecular mechanisms of neuronal apoptosis in the mammalian CNS. *Prog. Neurobiol.* **69**, 287-312.
Murgia, M., Hanau, S., Pizzo, P., Rippa, M. and Di Virgilio, F. (1993). Oxidized ATP. An irreversible inhibitor of the macrophage purinergic P2Z receptor. *J. Biol. Chem.* **268**, 8199-8203.
Newman, E. A. (2001). Propagation of intercellular calcium waves in retinal astrocytes and Muller cells. *J. Neurosci.* **21**, 2215-2223.
Newman, E. A. (2003). Glial cell inhibition of neurons by release of ATP. *J. Neurosci.* **23**, 1659-1666.
North, R. A. (2002). Molecular physiology of P2X receptors. *Physiol. Rev.* **82**, 1013-1067.
Oppenheim, R. W. (1991). Cell death during development of the nervous system. *Ann. Rev. Neurosci.* **14**, 453-501.
Perry, V. H., Henderson, Z. and Linden, R. (1983). Postnatal changes in retinal ganglion and optic axon populations in the pigmented rat. *J. Comp. Neurol.* **219**, 356-368.
Pettmann, B. and Henderson, C. E. (1998). Neuronal cell death. *Neuron* **20**, 633-647.
Rabacchi, S. A., Bonfanti, L., Liu, X. H. and Maffei, L. (1994). Apoptotic cell death induced by optic nerve lesion in the neonatal rat. *J. Neurosci.* **14**, 5292-5301.
Ralevic, V. and Burnstock, G. (1998). Receptors for purines and pyrimidines. *Pharmacol. Rev.* **50**, 413-492.
Raoul, C., Pettmann, B. and Henderson, C. E. (2000). Active killing of neurons during development and following stress: a role for p75(NTR) and Fas? *Curr. Opin. Neurobiol.* **10**, 111-117.
Raven, M. A., Eglen, S. J., Ohab, J. J. and Reese, B. E. (2003). Determinants of the exclusion zone in dopaminergic amacrine cell mosaics. *J. Comp. Neurol.* **461**, 123-136.
Reese, B. E. and Galli-Resta, L. (2002). The role of tangential dispersion in retinal mosaic formation. *Prog. Retinal Eye Res.* **21**, 153-168.
Reese, B. E., Harvey, A. R. and Tan, S.-S. (1995). Radial and tangential dispersion patterns in the mouse retina are cell-class specific. *Proc. Natl. Acad. Sci. USA* **92**, 2494-2498.
Reutelingsperger, C. P., Dumont, E., Thimister, P. W., van Genderen, H., Kenis, H., van de Eijnde, S., Heidendal, G. and Hofstra, L. (2002). Visualization of cell death in vivo with the annexin A5 imaging protocol. *J. Immunol. Methods* **265**, 123-132.
Rodieck, R. W. (1991). The density recovery profile: a method for the analysis of points in the plane applicable to retinal studies. *Vis. Neurosci.* **6**, 95-111.
Santos, P. F., Caramelo, O. L., Carvalho, A. P. and Duarte, C. B. (1999). Characterization of ATP release from cultures enriched in cholinergic amacrine-like neurons. *J. Neurobiol.* **41**, 340-348.
Stacy, R. C. and Wong, R. O. L. (2003). Developmental relationship between cholinergic amacrine cell processes and ganglion cell dendrites of the mouse retina. *J. Comp. Neurol.* **456**, 154-166.
Virginio, C., MacKenzie, A., Rassendren, F. A., North, R. A. and Surprenant, A. (1999). Pore dilation of neuronal P2X receptor channels. *Nat. Neurosci.* **2**, 315-321.
Wässle, H. and Riemann, H. J. (1978). The mosaic of nerve cells in the mammalian retina. *Proc. Royal Soc. London B* **200**, 441-461.
Wheeler-Schilling, T. H., Marquordt, K., Kohler, K., Guenther, E. and Jabs, R. (2001). Identification of purinergic receptors in retinal ganglion cells. *Brain Res. Mol. Brain Res.* **92**, 177-180.
Williams, R. W. and Herrup, K. (1988). The control of neuron number. *Annu. Rev. Neurosci.* **11**, 423-453.
Wong, R. O. (1999). Retinal waves and visual system development. *Annu. Rev. Neurosci.* **22**, 29-47.
Wong, R. O. and Collin, S. P. (1989). Dendritic maturation of displaced putative cholinergic amacrine cells in the rabbit retina. *J. Comp. Neurol.* **287**, 164-178.
Wong, R. O. and Godinho, L. (2003). Development of the vertebrate retina. In *The Visual Neurosciences*, vol. 1 (ed. L. M. Chalupa and J. S. Werner). Cambridge, MA: MIT Press.
Wu, D. K. and Cepko, C. L. (1993). Development of dopaminergic neurons is insensitive to optic nerve section in the neonatal rat retina. *Brain Res. Dev. Brain Res.* **74**, 253-260.
Zimmermann, H. (1996). Biochemistry, localization and functional roles of ecto-nucleotidases in the nervous system. *Prog. Neurobiol.* **49**, 589-618.